Landau level spectroscopy of ultrathin graphite layers

M.L. Sadowski, G. Martinez, and M. Potemski

Grenoble High Magnetic Field Laboratory, CNRS, Grenoble, France

C. Berger* and W.A. de Heer

Georgia Institute of Technology, Atlanta, Georgia, USA

(Dated: May 31, 2006)

Far infrared transmission experiments are performed on ultrathin epitaxial graphite samples in a magnetic field. The observed cyclotron resonance-like and electron-positron-like transitions are in excellent agreement with the expectations of a single-particle model of Dirac fermions in graphene, with an effective velocity of $\tilde{c} = 1.03 \times 10^6$ m/s.

The electronic properties of graphite have recently become the center of considerable attention, following the experiments on graphite monolayers (graphene) [1], including the discovery of an unusual sequence of quantum Hall effect states in such layers [2, 3]. The considerable interest in two-dimensional graphite is fuelled by its particular band structure and ensuing dispersion relation for electrons, leading to numerous differences with respect to "conventional" two-dimensional electron systems (2DES) [4, 5, 6, 7, 8, 9, 10, 11]. The band structure of graphene is considered to be composed of cones located at two inequivalent Brillouin zone corners at which the conduction and valence bands merge. In the vicinity of these points the electron energy depends linearly on its momentum: $E(\overrightarrow{p}) = \pm\tilde{c}|\overrightarrow{p}|$, which implies that free charge carriers in graphene are governed not by Schrödinger's equation, but rather by Dirac's equation for zero rest mass particles, with an effective velocity $\tilde{c}$, which replaces the speed of light. With the application of an external magnetic field, the Dirac energy spectrum evolves into Landau levels with energies given by

$$E_n = sgn(n)\tilde{c}\sqrt{2e\hbar B|n|} = sgn(n)E_1\sqrt{|n|} \qquad (1)$$

where n scans all positive (for electrons) and negative (for holes) integers and - very importantly - zero. E_1 may be understood as a characteristic energy introduced by the magnetic field. The square root dependence on B and Landau level index n is in stark contrast to "conventional" 2D electrons, where $E_n = (n+\frac{1}{2})\hbar eB/m, (n \geq 0)$, and the Landau levels are equally spaced.

The unusual sequence of quantum Hall effect states and an energy-dependent electron effective mass [2, 3], found in magneto-resistance measurements, are consistent with the model of Dirac particles. Here we report a magneto-spectroscopy study of the optical properties of ultrathin epitaxial graphite layers, in which we directly probe the dependence of the energy of electrons on their momentum.

The experiments were performed on graphene layers grown in vacuum by the thermal decomposition method [10], on single crystal (4H) SiC. These epitaxial graphene structures are routinely characterized using low energy electron diffraction, Auger electron spectroscopy, X-ray diffraction, scanning tunnelling microscopy and atomic force microscopy. The results of these measurements in combination with angular resolved photoelectron spectroscopy and transport data indicate that the active part of this type of structures consists of a few (3-5) graphene layers [10]. We investigated two such (unpatterned) structures, which both show a similar behavior, but in this Letter we present detailed studies for only one of them.

The far infra-red transmission of the samples was measured, at a temperature of 2K, as a function of the magnetic field B. A Si bolometer was placed directly beneath the sample to detect the transmitted radiation. The light (provided and analyzed by a Fourier transform spectrometer) was delivered to the sample by means of light-pipe optics. All experiments were performed with non-polarized light, in the Faraday geometry with the wave vector of the incoming light parallel to the magnetic field direction. The transmission spectra were normalized by the transmission of the substrate and by the zero-field transmission, thus correcting for magnetic field induced variations in the response of the bolometer. The SiC substrate used was completely opaque for energies between 85 meV and about 200 meV, which limited the range of our investigation.

The main experimental finding consists of several absorption lines visible in the spectra. A representative transmission spectrum, at 0.4 T, is shown in Fig. 1. These lines evolve spectacularly with the magnetic field. Two main lines are shown in Fig. 2 for several values of the field. As shown in Fig. 3, their energies, plotted as a function of the square root of the magnetic field, trace perfect straight lines, in excellent agreement with eq. 1. Also shown in this figure are the energy positions of the two other lines. Experiments performed in a tilted configuration show that the position of the transition line (filled symbols in Fig. 3) depends only on the component of the magnetic field perpendicular to the sample plane.
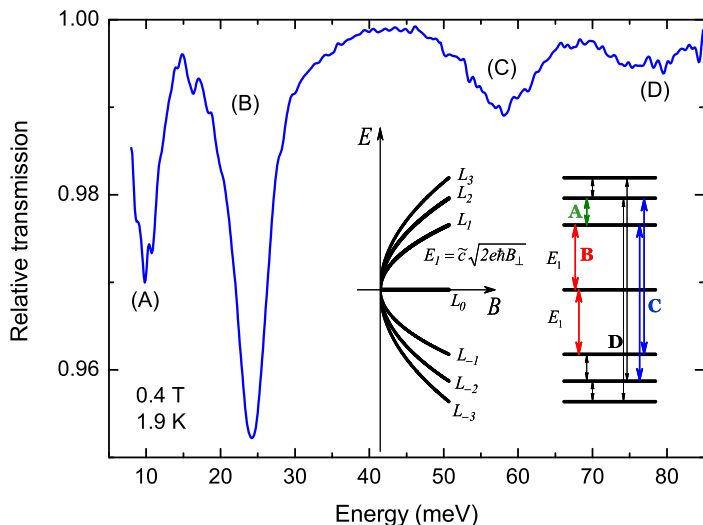
---

*also at LEPES, CNRS Grenoble, France

FIG. 1: (Color online) Relative transmission trace at 0.4 T and 1.9 K shows 4 distinct transitions. The assignations are (see text) A: $L_1 \rightarrow L_2$, B: $L_0 \rightarrow L_1(L_{-1} \rightarrow L_0)$, C : $L_{-2} \rightarrow L_1(L_{-1} \rightarrow L_2)$, D: $L_{-3} \rightarrow L_2(L_{-2} \rightarrow L_3)$. The inset shows a schematic of the evolution of Landau levels with applied magnetic field, and possible optical transitions.

FIG. 2: (Color online) Development of two main transmission lines with the magnetic field. Upper panel shows the line marked C in Fig.1, corresponding to $L_{-1} \rightarrow L_2(L_{-2} \rightarrow L_1)$ transitions, lower panel shows the line marked B, corresponding to $L_0 \rightarrow L_1(L_{-1} \rightarrow L_0)$ transitions

A complicated structure at still lower energies, not shown in the figure, moving slowly to higher energies with magnetic field, was also observed. Unusually, the intensities of the two main lines increase markedly with increasing magnetic field, with the lower-energy line always remaining stronger.

Cyclotron resonance in graphite was studied a long time ago both experimentally [12] and theoretically [13, 14]. While the resonant magnetic field was also found to scale with the cosine of the angle between the field and the graphene planes, these experiments were well described by a linear dependence of the cyclotron frequency ω_C on the magnetic field, with an effective mass of $0.058 m_0$. Our results are best described using the theoretical predictions of a simple single-particle (Dirac) model for a graphene layer, and we will use this language in the following paragraphs. To facilitate the discussion, we sketch the graphene Landau levels and possible transitions between them in the inset to Fig. 1.

Thus, we assign the strongest line to the transitions to and from the lowest Landau level. Note that, since the conduction and valence band states in graphene are built from the same atomic orbitals, the positive and negative branches of the dispersion relation are identical. The ensuing symmetry means that the $L_0 \rightarrow L_1$ and $L_{-1} \rightarrow L_0$ transitions are indistinguishable in an experiment using unpolarized radiation.

A straight line fit of the points corresponding to this transition using the expression $E = E_1 = \tilde{c}\sqrt{2e\hbar B}$ yields a very accurate value for $\tilde{c}$, the velocity of electrons in graphene, which replaces the speed of light in the dispersion relation viewed in terms of Dirac's formalism. This is found to be $(1.03 \pm 0.01) \times 10^6$ m/s, close to those used
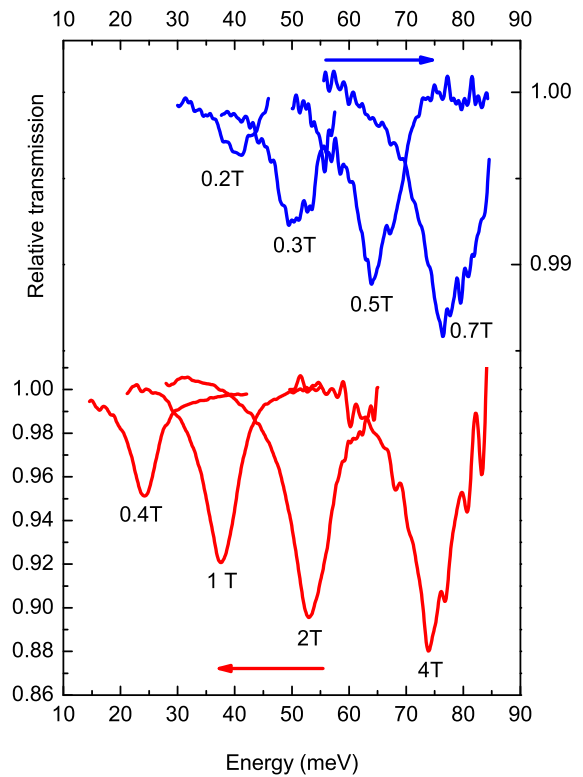
in the interpretation of Hall effect measurements [2, 3].

The slopes of the other lines traced in Fig. 3, starting from the highest energy transition, scale exactly as $(\sqrt{3} + \sqrt{2}) : (\sqrt{2} + 1) : 1 : (\sqrt{2} - 1)$, allowing these lines to be assigned to transitions $L_{-2} \rightarrow L_3(L_{-3} \rightarrow L_2)$, $L_{-1} \rightarrow L_2(L_{-2} \rightarrow L_1)$, $L_0 \rightarrow L_1(L_{-1} \rightarrow L_0)$, and $L_1 \rightarrow L_2$, respectively, as shown in the figure.

The fact that transitions involving the L_0 Landau level are visible at such low magnetic fields places an upper limit on the electron concentration in the observed layer. The observation of the $L_0 \rightarrow L_1(L_{-1} \rightarrow L_0)$ line implies the existence of unpopulated states at least on the L_1 level. This line is clearly observed at fields $B \approx 0.15$ T, and therefore the L_1 level can be fully populated only when $B < 0.15$ T. Thus $n \leq 2.1 \times 10^{10}$ cm^{-2} (where we take into account the 2- and 4-fold degeneracy of the L_0 and L_1 electronic Landau levels, respectively).

We now turn our attention to the strength of the transitions. As may be seen in Fig. 2, both the main transitions gain in intensity with increasing magnetic field. To better visualize this trend, we plot the integrated intensity (area under the dip in the relative transmission) as a function of the square root of the magnetic field (Fig. 4).

The relative transmission of a sheet of conducting electrons between vacuum and a dispersionless polar medium
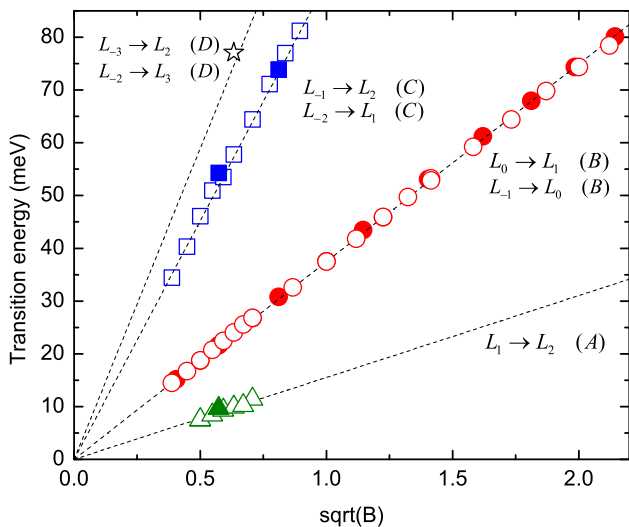
FIG. 3: The observed transitions, together with their assignments, plotted versus $B_\perp$. The filled symbols are data obtained for the sample tilted with respect to the direction of B by an angle of 50^0. The dashed lines are all calculated with the same characteristic velocity $\tilde{c} = 1.03 \times 10^6$ m/s.

FIG. 4: Area of the main peak observed in the experiments - the $L_0 \to L_1 (L_{-1} \to L_0)$ transition - plotted against the square root of the magnetic field. The line is traced using the expression $\beta(e^2/2\epsilon_0 \hbar c)E_1$.

with a refractive index n, for unpolarized radiation and in the limit of weak absorption, may be written as (see e.g. [15, 16])

$$T(\omega, B) \approx 1 - \beta \frac{Re(\sigma_{xx}(\omega, B))}{\epsilon_0 c}$$

where $\sigma_{xx}(\omega, B)$ is a diagonal element of the optical conductivity tensor, ϵ_0 is the vacuum permittivity, c is the speed of light in vacuum and $\beta = (n^2+3)/2(n^2+1) = 0.63$ for SiC, where n=2.6 [17]. The optical conductivity of the two-dimensional electrons may be written using the Kubo formalism [18] and taking into account the properties of the graphene Landau level wave functions [7, 19]

$$\sigma_{xx}(\omega, B) = \frac{4G_B e^2}{\omega} \sum_{m,n} \frac{(f_m - f_n)M_{m,n}}{E_{m,n} - (\hbar\omega + i\gamma)}$$

where $E_{m,n}$ are the transition energies between levels m and n, $G_B = eB/h$ is the Landau level degeneracy, f_m, f_n are the occupancies of the relevant Landau levels and the selection rules for the optically active transitions are given by $M_{m,n} = (\tilde{c}^2/p)\delta_{|m|,|n|\pm 1}$, with p = 2 for m or n =0 and 4 otherwise. The summation is performed over all Landau levels m, n, and the fourfold degeneracy of each Landau level has already been accounted for.

The integrated transmission for a single transition between a completely filled (L_0) and a completely empty (L_1) Landau level, using the above expression (for linewidths γ small compared to the transition energy) may be written as:

$$I(B) = \frac{1}{\epsilon_0 c}\int Re(\sigma_{xx}(\omega))d\omega \approx \frac{e^3 \tilde{c} B}{\epsilon_0 c E_1} = \beta \frac{e^2}{2\epsilon_0 \hbar c}E_1$$
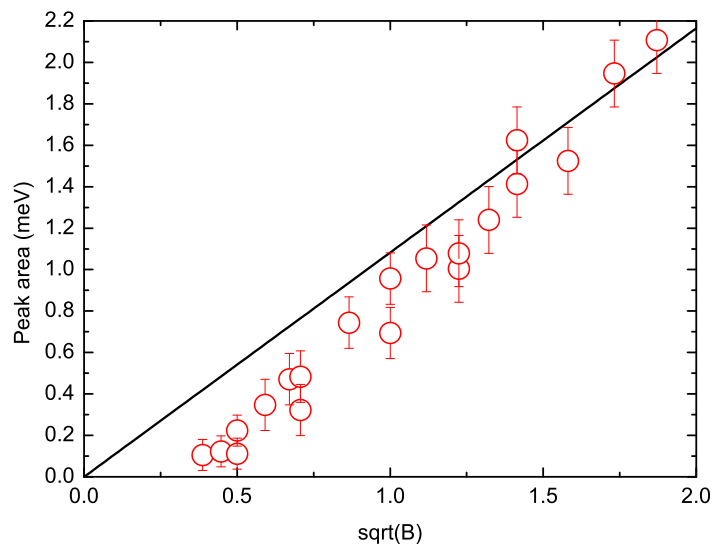
where E_1 is the characteristic energy introduced earlier.

The above equation gives a rough estimate of the intensity of the strongest transition, in the range of high magnetic fields where the Fermi energy is pinned to the L_0 level. This is due to the fact that the decreasing intensity of the $L_0 \to L_1$ transition is compensated by the corresponding increase of the strength of the superimposed $L_{-1} \to L_0$ transition. In spite of the rather crude approximation, Fig. 4 indeed shows that the observed transition follows the expected trend; the good agreement of the absolute measured and calculated values is another factor supporting the picture of a single, possibly inhomogeneous, graphene layer (see discussion in following paragraphs).

Several notable differences emerge between Dirac electrons and conventional two-dimensional electron (2DEG) systems, such as those present for instance in GaAs heterojunctions. As we have shown, transitions between adjacent Landau levels in graphene occur at markedly different energies (for example $L_0 \to L_1$ and $L_1 \to L_2$, Figs. 1 and 3). For a standard 2DEG, transitions between such pairs of Landau levels all have the same energy. More striking, a different class of transitions, with no counterpart in a standard 2DEG, is observed in graphene and involves those from filled hole states $(n < 0)$ to empty electron states $(n > 0)$ (e.g. our $L_{-1} \to L_2$ and $L_{-2} \to L_1$ transitions). These are the particle-antiparticle creation and annihilation events in the Dirac formalism.

Since some of the observed transitions may be considered as analogues of cyclotron resonance excitations, it is tempting to look at them in a semi-classical context, using the concept of an effective mass. While for a conventional 2DEG, with a quadratic dispersion law, there

is a coincidence between classical and quantum mechanical solutions of the optically active response in a magnetic field, this does not hold for graphene. The classically derived cyclotron excitation E_C in this system is $E_C = \hbar eB/(E/\tilde{c}^2)$ [7], where E is the electron energy and $(E/\tilde{c}^2)$ stands for the electron mass - energy and mass being equivalent in the relativistic picture. Although the effective rest mass of the electrons in graphene is zero, their energy-dependent cyclotron mass - which will also change with magnetic field - can be followed down to the lowest energies ($\simeq 7$ meV in our case), giving a cyclotron effective mass down to 0.0012 m_0.

All the experimental results cited above are consistent with the expected behavior of zero effective rest mass Dirac fermions. Having demonstrated the presence of such carriers in the investigated structure, let us now consider the following points: (i) linear dispersion has so far been demonstrated only for single layers; (ii) our structure is known to contain several graphene layers; (iii) Hall effect measurements on the same samples show concentrations of the order of 10^{12} cm^{-2}, while our results point to a concentration two orders of magnitude smaller; (iv) a graphene bilayer [20, 21] is found to exhibit parabolic dispersion; (v) several graphene layers [22] may, depending on the stacking scheme, exhibit linear and/or parabolic dispersion relations.

The concentration discrepancy may be explained as follows. As usual at the interfaces, the electric field induced by the surface charge compensates for the work function difference between SiC and graphene. Due to the abrupt change of the built-in electric field, the interface monolayer has a high carrier concentration, which decreases away from the interface: while the Fermi energy in the first monolayer is located high in the conduction band, it may be quite close to the Dirac point for other layers. A mesoscopic sample patterned on the same wafer as our selected sample has been investigated in transport experiments which also show the unusual quantum Hall effect in epitaxial graphene. It is believed that these transport experiments probe the interface layer in which the estimated electron sheet concentration is $\simeq 4 \times 10^{12} cm^{-2}$. In contrast, our transmission experiments probe the whole sequence of layers, among them also those which are quasi-neutral. The previously mentioned very low-energy features in our spectra probably arise from the high-electron-concentration parts of the sample, where the energy difference between adjacent Landau levels is small.

Another factor possibly affecting the data could be lateral inhomogeneity, i.e. fluctuations in the electron concentration, within a single graphene plane. Finally, individual graphene planes in epitaxial graphite may be much more weakly coupled than is usually accepted for graphite. The current experiment shows an absorption in good agreement with that expected for graphene, but the simple approximation used may be insufficient to definitely distinguish between one and a few (inhomogeneous) uncoupled layers.

Concluding, we have measured the optical excitation spectrum of Dirac fermions - to the best of our knowledge, the first such measurement in a condensed matter system. These fermions are found in thin layers of epitaxial graphite, most probably in the form of single (or extremely weakly coupled) graphene layers (or parts of layers). These excitations are very well described in terms of a relativistic-like Dirac hamiltonian. Cyclotron resonance like transitions coexist with electron-hole (particle-antiparticle) like transitions, with energy positions and oscillator strengths in surprisingly good agreement with expectations based on a model of non-interacting particles with linear dispersion.

[1] K. S. Novoselov, A. K. Geim, S. V. Morozov, D. Jiang, Y. Zhang, S. V. Dubonos, I. V. Grigorieva, and A. A. Firsov, Science **306**, 666 (2004).

[2] K. S. Novoselov, A. K. Geim, S. V. Morozov, D. Jiang, M. I. Katsnelson, I. V. Grigorieva, S. V. Dubonos, and A. A. Firsov, Nature **438**, 197 (2005).

[3] Y. Zhang, Y.-W. Tan, H. L. Stormer, and P. Kim, Nature **438**, 201 (2005).

[4] P. R. Wallace, Phys. Rev. **71**, 622 (1947).

[5] J. W. McClure, Phys. Rev. **104**, 666 (1956).

[6] F. D. M. Haldane, Phys. Rev. Lett. **61**, 2015 (1988).

[7] Y. Zheng and T. Ando, Phys. Rev. B **65**, 245420 (2002).

[8] V. P. Gusynin and S. G. Sharapov, cond-mat/0512157.

[9] N. M. R. Peres, F. Guinea, and A. H. Castro Neto, Phys. Rev. B **73**, 125411 (2006).

[10] C. Berger, Z. Song, T. Li, X. Li, A. Y. Ogbazghi, R. Feng, Z. Dai, A. N. Marchenkov, E. H. Conrad, P. N. First, et al., J. Phys. Chem. **108**, 19912 (2004).

[11] C. Berger, Z. Song, T. Li, X. Li, X. Wu, N. Brown, C. Naud, D. Mayou, A. N. Marchenkov, E. H. Conrad, et al., Science **312**, 1191 (2006).

[12] J. K. Galt, W. A. Yager, and J. H. W. Dail, Phys. Rev. **103**, 1586 (1956).

[13] P. Nozières, Phys. Rev. **109**, 1510 (1958).

[14] M. Inoue, J. Phys. Soc. Jpn. **17**, 808 (1962).

[15] K. W. Chiu, T. K. Lee, and J. J. Quinn, Surf. Sci. **58**, 182 (1976).

[16] T. Ando, J. Phys. Soc. Jpn. **38**, 989 (1975).

[17] Y. Goldberg, M. E. Levinshtein, and S. L. Rumyantsev, *Properties of Advanced Semiconductor Materials GaN, AlN, SiC, BN, SiC, SiGe* (John Wiley & Sons, Inc., New York, 2001), pp. 93–148.

[18] R. Kubo, J. Phys. Soc. Jpn. **12**, 570 (1957).

[19] T. Ando, Y. Zheng, and H. Suzuura, J. Phys. Soc. Jpn.

71, 1318 (2002).

[20] E. McCann and V. I. Fal'ko, Phys. Rev. Lett. **96**, 086805 (2006).

[21] K. S. Novoselov, E. McCann, S. V. Morozoz, V. I. Fal'ko, M. I. Katsnelson, U. Zeitler, D. Jiang, F. Schedin, and A. K. Geim, Nature Physics **2**, 177 (2006).

[22] F. Guinea, A. H. Castro Neto, and N. M. R. Peres, cond-mat/0604396.